Constraints on Asian and European sources of methane from CH 4 -C 2 H 6 -CO correlations in Asian outflow

Citation	Xiao, Yaping, Daniel J. Jacob, James S. Wang, Jennifer A. Logan, Paul I. Palmer, Parvadha Suntharalingam, Robert M. Yantosca, Glen W. Sachse, Donald R. Blake, and David G. Streets. 2004. "Constraints on Asian and European Sources of Methane from CH 4 -C 2 H 6 - CO Correlations in Asian Outflow." Journal of Geophysical Research 109, issue D15.
Published Version	doi:10.1029/2003JD004475
Citable link	http://nrs.harvard.edu/urn-3:HUL.InstRepos:14117724
Terms of Use	This article was downloaded from Harvard University's DASH repository, and is made available under the terms and conditions applicable to Open Access Policy Articles, as set forth at http://nrs.harvard.edu/urn-3:HUL.InstRepos:dash.current.terms-of-use#OAP

Constraints on Asian and European sources of methane from CH_4 - C_2H_6-CO correlations in Asian outflow

Yaping Xiao, Daniel J. Jacob, James S. Wang*, Jennifer A. Logan, Paul I. Palmer, Parvadha Suntharalingam, Robert M. Yantosca
Department of Earth and Planetary Sciences and Division of Engineering and Applied Sciences, Harvard University, Cambridge, MA

Glen W. Sachse
NASA Langely Research Center, Hampton, VA

Donald R. Blake
Department of Chemistry, University of California, Irvine, CA

David G. Streets
Argonne National Laboratory, Argonne, IL

*now at Environmental Defense, New York, NY

Short title: Asian and European methane sources

Abstract. Aircraft observations of Asian outflow from the TRACE-P aircraft mission over the NW Pacific (March-April 2001) show large CH_4 enhancements relative to background, as well as strong CH_4-C_2H_6-CO correlations that provide signatures of regional sources. We apply a global chemical transport model simulation of the CH_4-C_2H_6-CO system for the TRACE-P period to interpret these observations in terms of CH_4 sources, and to explore in particular the unique constraints from the CH_4-C_2H_6-CO correlations. We use as a priori a global CH_4 source inventory constrained with NOAA/CMDL surface observations [*Wang et al.,* 2003]. We find that the observed CH_4 concentration enhancements and CH_4-C_2H_6-CO correlations in Asian outflow in TRACE-P are determined mainly by anthropogenic emissions from China and Eurasia (defined here as Europe + eastern Russia), with only little contribution from tropical sources (wetlands and biomass burning). The a priori inventory overestimates the observed CH_4 enhancements and shows regionally variable biases for the CH_4/C_2H_6 slope. The CH_4/CO slopes are simulated without significant bias. Matching both the observed CH_4 enhancements and the CH_4-C_2H_6-CO slopes in Asian outflow requires increasing the East Asian anthropogenic source of CH_4, and decreasing the Eurasian anthropogenic source, by at least 30% for both. The need to increase the East Asian source is driven by the underestimate of the CH_4/C_2H_6 slope in boundary layer Chinese outflow. The *Streets et al.* [2003] anthropogenic emission inventory for East Asia fits this constraint by increasing CH_4 emissions from that region by 40% relative to the a priori, largely because of higher livestock and landfill source estimates. Eurasian sources (mostly European) then need to be reduced by 30-50% from the a priori value of 68 Tg yr^{-1}. The decrease of European sources could result in part from recent mitigation of emissions from coal mining and landfills.

1. *Introduction*

Atmospheric methane (CH_4) is an important greenhouse gas with an atmospheric lifetime of about 10 years. The atmospheric abundance of CH_4 has increased by a factor of 2.5 since pre-industrial times [*Etheridge et al.,* 1998]. The resulting radiative forcing is half that of CO_2 [*Hansen and Sato,* 2000]. Methane also plays a central role in atmospheric chemistry. It is an important sink for tropospheric OH and hence affects the oxidizing power of the atmosphere. It is a major source of tropospheric ozone, with implications for both the oxidizing power of the atmosphere and air quality [*Fiore et al.,* 2002]. Methane affects stratospheric ozone both by scavenging Cl radicals and by providing a source of water vapor. Better understanding of anthropogenic influences on CH_4 is essential for addressing issues of climate change and global atmospheric chemistry.

Considerable research has focused on quantifying sources of CH_4 [*IPCC* 2001]. The major anthropogenic sources include rice cultivation, livestock, landfills, fossil fuel production and consumption (natural gas venting, leakage and coal mining), and biomass burning. The major natural sources include wetlands and termites. The total emission from all sources is known to be in the range 460-600 Tg yr^{-1} because of independent constraints from halocarbon data on the global mean tropospheric OH concentration, and hence on the CH_4 sink [*Prinn et al.,* 1995, 2001; *Spivakovsky et al,* 2000]. However, estimates for most of the individual source terms in the global CH_4 budget have uncertainties of a factor of two or more according to *IPCC* [2001]. Better understanding of these individual source terms and their contributions to the long-term trend in CH_4 is needed.

The traditional approach for estimating CH_4 sources has been by global extrapolation from limited flux measurements and socioeconomic data [e.g., *Matthews et al.,* 1987, 1991*; Lerner et al.,* 1988; *Cicerone and Oremland,* 1988]. These bottom-up emission inventories suffer from substantial uncertainty due to under-sampling of the sources and poor characterization of source variability. Global chemical transport model (CTM) simulations of atmospheric CH_4 observations from the NOAA/CMDL network of surface sites have been used to test the bottom-

up emission inventories, either by a forward model with multiple scenarios [*Fung et al.,* 1991] or by formal inverse modeling methods [*Hein et al.,* 1997*; Houweling et al.,* 1999*; Wang et al.,* 2003; *Mikaloff Fletcher et al.,* 2004]. However, spatial overlap of the sources makes it difficult to derive a unique set of top-down constraints for CH_4 sources from the limited surface air observations. Additional constraints on the CH_4 budget and specific sources are provided by measurements of the carbon isotopes $\delta^{13}C$ and $^{14}CH_4$ [*Lowe et al.,* 1991, 1994; *Gupta et al.,* 1996; *Quay et al.,* 1999; *Miller et al.,* 2002; *Mikaloff Fletcher et al.,* 2004], but these data are even more limited.

We show here that improved top-down constraints on the sources of CH_4 can be obtained from observations of CH_4-C_2H_6-CO correlations interpreted with a global CTM. Ground-based and aircraft measurements show strong correlations of CH_4 with C_2H_6 and CO [*Harriss et al.,* 1994; *Blake et al.,* 1996; *Bartlett et al.,* 1996; *Shipham et al.,*1998; *Matsueda et al.,* 1999]. Ethane (C_2H_6) is a tracer of natural gas leakage, coal mining, and biomass burning [*Rudolph,* 1995]. CO is a general tracer of combustion. Both C_2H_6 and CO have atmospheric lifetimes of a few months, sufficiently long to serve as atmospheric tracers of their sources. One might therefore expect the biomass burning source of CH_4 to have a correlated CH_4-C_2H_6-CO signature, the natural gas/oil/coal mining sources to have a correlated CH_4-C_2H_6 signature, and the sources from livestock, rice cultivation, landfills and wetlands to have no direct correlations with CO and C_2H_6. In practice, co-location of these different sources complicates the interpretation, and a CTM analysis is needed.

We focus our analysis here on CH_4-C_2H_6-CO correlations in Asian outflow, using observations from the NASA TRACE-P aircraft mission over the western Pacific during March-April 2001 [*Jacob et al.,* 2003]. Asia is of particular interest as a source of CH_4 due to its large population, rapid industrialization, and extensive rice cultivation. There is also considerable seasonal biomass burning in Southeast Asia in spring [*Duncan et al.,* 2003a]. The TRACE-P mission used two aircraft, based in Hong Kong and Japan, to characterize the chemical composition of Asian outflow. The major outflow pathways involved frontal lifting by warm conveyor belts (WCBs) ahead of southeastward-moving cold fronts, and boundary layer

advection behind the cold fronts [*Fuelberg et al.,* 2003; *Liu et al.,* 2003a]. *Bartlett et al.* [2003] reported strong correlations of CH_4 with C_2H_6, ethyne (C_2H_2), propane (C_3H_8), and carbon tetrachloride (C_2Cl_4) in the Asian outflow. They concluded that urban and combustion sources dominated the regional CH_4 budget. However, a bottom-up inventory of Asian CH_4 sources for 2000 generated by *Streets et al.* [2003] in support of TRACE-P identified livestock, landfills, rice cultivation, coal mining, and biomass burning as the principal regional sources of CH_4, in apparent contradiction with the analysis of *Bartlett et al.* [2003]. The *Streets et al.* [2003] inventory also includes estimates of C_2H_6 and CO emissions, allowing a consistent interpretation of observed TRACE-P correlations using a CTM simulation.

We use here the GEOS-CHEM CTM [*Bey et al.,* 2001a] in a consistent simulation of the CH_4-C_2H_6-CO system for the TRACE-P period. This model has been used previously for global simulations of CH_4 and CO aimed at understanding trends in the past decade [*Wang et al.,* 2003; *Duncan et al.,* 2003b]; Previous GEOS-CHEM applications to the analysis of TRACE-P data included investigation of Asian outflow pathways [*Liu et al.,* 2003a] and transpacific transport [*Heald et al.,* 2003b*; Jaegle et al.,* 2003], as well as quantification of the Asian sources of CO [*Palmer et al.,* 2003a*; Heald et al,* 2003a], CO_2 [*Suntharalingam et al.,* 2003], nitriles [*Li et al.,* 2003], halocarbons [*Palmer et al.,* 2003b], and ozone [*Liu et al.,* 2003b]. Transport in the model is thus heavily diagnosed for the TRACE-P period, and there are no systematic biases [*Kiley et al.,* 2003]

2. *Model description*

2.1. *General description*

The GEOS-CHEM CTM (http://www.as.harvard.edu/chemistry/trop/geos/index.html, v4.26) is driven by assimilated meteorological fields from the Goddard Earth Observing System (GEOS) of the NASA Global Modeling and Assimilation Office (GMAO). We use GEOS-3 meteorological fields for the TRACE-P time period with a horizontal resolution of 1° x 1°, 48 vertical sigma levels up to 0.01hPa, and a temporal resolution of 6 hours (3 hours for surface

variables and mixed layer depths). The horizontal resolution is degraded here to 2 $^{\circ}$ latitude by 2.5° longitude for computational expediency.

The main sinks of CH_4, CO and C_2H_6 are reactions with OH. The rate constants are from *Demore et al.* [1997]. For CH_4, we also include a minor sink from soil absorption (about 30 Tg yr^{-1}) [*Wang et al.,* 2003]. Global 3-D monthly mean tropospheric OH concentrations from a full tropospheric oxidant simulation (GEOS-CHEM v4.33) are used [*Fiore et al.,* 2003]. These OH concentrations yield an annual mean methyl chloroform (CH_3CCl_3) lifetime against loss by tropospheric OH of 6.3 years, which is within the range of 5.3-6.9 years estimated by *Prinn et al.* [2001] from CH_3CCl_3 measurements. The same OH fields have been used in other GEOS-CHEM simulations of the TRACE-P data [*Li et al.,* 2003; *Heald et al.,* 2003a, b*; Jaegle et al.,* 2003*; Palmer et al.,* 2003a].

Tagged tracer simulations for CH_4, C_2H_6 and CO in GEOS-CHEM are conducted to quantify the contributions to atmospheric concentrations from different source regions and source types. These tagged tracer simulations all use the same OH concentrations as the standard simulation, so that results are additive. Source regions include East Asia, Europe, eastern Russia, North America, and the rest of the world as defined in Figure 1. We will refer to "Eurasia" as the combination of Europe and eastern Russia. Source types for CH_4 include livestock, rice cultivations, wetlands, biomass burning, biofuels, fossil fuel (gas/oil/coal mining), and landfills. The simulations of C_2H_6 and CO are initialized with a two-year spin-up. The initialization of the CH_4 simulation is described in section 2.3.

2.2. Emissions

2.2.1 Methane

We use the global 1998 inventory of *Wang et al.* [2003] as our a priori estimate of CH_4 emissions. The global CH_4 growth rate was near zero between 1998 and 2001, presumably reflecting a leveling off of emissions [*Dlugokencky et al.,* 1998], although a positive trend of global OH concentrations could have contributed. *Wang et al.* [2003] originally derived their

inventory for 1994 by inverse analysis of the NOAA/CMDL surface observations, using GEOS-CHEM as the forward model, and then applied interannual variability to these emissions for 1988-1998 on the basis of socioeconomic and meteorological data. They found that they could capture in this manner much of the observed spatial and temporal variability of CH_4 concentrations over the 1988-1997 decade.

Table 1 summarizes the global and East Asian CH_4 sources from *Wang et al.* [2003] and compares them to the global EDGAR3.2 emission inventory [*Olivier,* 2001a] and to the East Asian emission inventory of *Streets et al.* [2003]. The latter two inventories include only anthropogenic sources and biomass burning. Anthropogenic sources here include rice cultivation, livestock, fossil fuel (gas/oil/coal mining), landfills, and biofuel. Classifying the biomass burning source as natural or anthropogenic is somewhat subjective. For the purpose of this paper we will regard it as natural, largely out of convenience since its geographical distribution (mainly tropical) is distinct from that of the major anthropogenic sources. Annual East Asian emissions in the *Wang et al.* [2003] inventory are dominated by wetlands, rice cultivation, livestock (including animal enteric fermentation and animal waste management), coal mining, and landfills. Natural gas and biofuel sources are relatively small. We refer to the sum of natural gas (production and transmission), oil (production, transmission and handling), and coal mining as the fossil fuel source. The other fossil fuel sources of CH_4 from industry, power generation, residential and commercial use, and transport are all minor [*Olivier,* 2001a].

East Asian emissions from rice cultivation in the *Streets et al.* [2003] inventory are 50% lower than in *Wang et al.* [2003] and the coal mining source is 40% lower, while livestock emissions are 30% higher and landfill emissions are a factor of two higher. The EDGAR3.2 inventory is better aligned with *Streets et al.* [2003].

Seasonal variation of CH_4 emissions from rice cultivation, biomass burning, and wetlands is applied here following *Wang et al.* [2003]. Our focus is on the February-April (TRACE-P) period. East Asian emissions from rice cultivation peak in June-October (170% of annual mean flux) and are low during February-April (40% of annual mean flux). This is consistent with the *Streets et al.* [2003] inventory in which CH_4 emissions from rice cultivation peak in fall and are

low in spring. Emissions from natural wetlands in February-April are about 80% of the annual average. Biomass burning in Southeast Asia is by contrast at its seasonal high (240% of annual mean flux) during February-April.

Figure 2 shows the geographical distribution of CH_4 emissions for February-April 2001 in the *Wang et al.* [2003] inventory. There are important regional differences between sources. In China and India the major sources are livestock, coal mining, landfills, and rice cultivation. Landfills and gas/oil are the main sources in Japan. Wetlands, rice cultivation, biomass burning, and livestock are important sources in Southeast Asia. Fossil fuel (mostly from natural gas), landfills, and livestock are dominant in Eurasia.

2.2.2. Ethane

Major sources of C_2H_6 include natural gas leakage, natural gas venting, coal mining, biofuel use, and biomass burning [*Rudolph,* 1995]. We refer to the sum of the first three sources as the fossil fuel source. Anthropogenic emissions (fossil fuel and biofuel) for East Asia are taken from *Streets et al.* [2003]. Fossil fuel emissions for the rest of the world are scaled to the corresponding source of CH_4, for which better a priori information is available. Biofuel emissions for the rest of the world are based on the *Yevich and Logan* [2003] biofuel inventory with emission factors from *Andreae and Merlet* [2001]. Biomass burning emissions are scaled to the corresponding emission of CO [*Duncan et al.,* 2003a], with a C_2H_6/CO emission ratio dependent on fuel type [*Staudt et al.,* 2003].

Natural gas composition varies with geographical region [*Rudolph et al.,* 1995]. In this work, CH_4/C_2H_6 emission factors for the fossil fuel sources outside East Asia were derived by fitting the global C_2H_6 simulation to atmospheric concentration data including surface sites, ship cruises, aircraft missions, and total columns from ground-based remote sensing. We thus adopt molar CH_4/C_2H_6 emission ratios from fossil fuel of 8 in eastern Russia, 24 in Europe, and 19 for the rest of the world except East Asia, where the use of *Streets et al.* [2003] inventory for C_2H_6 yields a molar CH_4/C_2H_6 emission ratio of 40. These values are highly variable but roughly in the range of U.S. energy industry data [*Flores et al.,* 1999] which indicate emission ratios of 38

or higher (dry gas), 19-37 (gas condensate), and 11-18 (oil). Measurements in Chinese cities indicate CH_4/C_2H_6 concentration ratios in the range of 5-35 [Donald R. Blake, unpublished data]. Our total global C_2H_6 source of 13.5 Tg yr^{-1} (Table 2) is consistent with previous literature estimates of 8-24 Tg yr^{-1} [*Blake and Rowland,* 1986*; Kanakidou et al.,* 1991; *Rudolph,* 1995; *Boissard et al.,* 1996; *Gupta et al.,* 1998; *Wang et al.,* 1998].

2.2.3. Carbon monoxide

Our CO simulation for the TRACE-P period is that of *Palmer et al.* [2003a], who conducted an inverse model analysis of Asian CO sources on the basis of the TRACE-P CO observations. They used *a priori* inventories from *Streets et al.* [2003] for East Asian anthropogenic sources (fossil fuel and biofuel combustion), *Heald et al.* [2003a] for biomass burning in Southeast Asia, and *Duncan et al.* [2003a] for other sources. Transport was simulated with GEOS-CHEM, which served as the forward model for the inversion. Fitting the CO observations in TRACE-P required a 54% increase in anthropogenic emissions from China relative to the *a priori*, constrained by the observations in boundary layer outflow, and a 74% decrease in emissions from Southeast Asia (mostly from biomass burning), constrained by the observations in the free troposphere south of 30°N. Similar results for CO emissions were obtained by *Heald et al.* [2003b] from an analysis of MOPITT satellite observations of CO columns during the TRACE-P period. The optimized a priori sources of CO from *Palmer et al.* [2003a] are given in Table 2. The resulting simulation of CO concentrations, which we use here, is compared to TRACE-P observations in that paper. The mean bias is -4 ppb and the frequency distribution of differences is peaked around zero.

2.2.4. Emission ratios

Table 2 gives the CH_4-C_2H_6-CO emission ratios from selected sources, globally and for the two main source regions contributing to the structure of Asian outflow over the Pacific during TRACE-P: East Asia and Eurasia (Europe + eastern Russia). We exclude India from East Asia here since India did not contribute significantly to the structure of Asian outflow during the

TRACE-P period [*Palmer et al.,* 2003a]. There is substantial spatial overlap between the different anthropogenic sources of CH_4 (Figure 2), hence we also give for each region in Table 2 the lumped anthropogenic emission ratio.

Within East Asia, the CH_4/C_2H_6 emission ratio for fossil fuel (40 molar) is higher than that for biofuels (10) and close to that for biomass burning (35). The C_2H_6 emission factor for biofuels is much higher than for open biomass burning [*Bertschi et al.,* 2003], apparently because of preferential ethane production during flaming combustion [*Yokelson et al.,* 2003]. The CH_4/CO emission ratio for fossil fuel (0.30 molar) is 2-3 times that for biofuels (0.10) and biomass burning (0.12). The C_2H_6/CO emission ratio from fossil fuel (7.6×10^{-3} molar) is lower than that for biofuels (10×10^{-3}), but much higher than that for biomass burning (3.6×10^{-3}). The CH_4/CO and CH_4/C_2H_6 emission ratios from all lumped anthropogenic sources are larger than those from the combustion sources due to additional CH_4 inputs from livestock, landfills, and rice cultivation.

The CH_4 and C_2H_6 anthropogenic emissions from Eurasia are larger than from East Asia while the CO source is much smaller, reflecting more vigorous pollution control of CO and greater natural gas production in Eurasia. There are thus large differences in the CH_4/CO and C_2H_6/CO emission ratios for anthropogenic sources from East Asia vs. Eurasia (0.57 vs. 1.0 for CH_4/CO, 8.8×10^{-3} vs. 27×10^{-3} molar for C_2H_6/CO), and the CH_4/C_2H_6 anthropogenic emission ratio is larger for East Asia (64 vs. 37).

2.3. *Initialization and global aspects of the CH_4 simulation*

Proper model initialization of the CH_4 tagged tracers presents a difficulty because of the long lifetime of CH_4. We wish to use these tracers to interpret the variability of CH_4 in Asian outflow during March-April 2001. Because the time scale for mixing within the northern hemisphere is a few months, we expect the variability observed in TRACE-P to reflect fresh emissions from the past 2-3 months together with the latitudinal and vertical structure of the background. Accordingly we define a background CH_4 tracer in the simulation as the CH_4 present in the atmosphere on January 1, 2001, including contributions from all sources. This

background tracer has no emissions following January 1 and is allowed to decay by oxidation by OH. The other tagged tracers, representing different CH_4 source regions and source types, are initialized with zero concentration on January 1. They build up over the course of the simulation as a result of emissions and are removed by oxidation by OH. The same archived OH concentration fields are used to calculate the losses of all tracers, hence the sum of the individual tracers adds up to the total CH_4 concentration.

We need to define a global field for the background tracer on January 1, 2001. We start from NOAA/CMDL global surface observations for December 2000 [ftp://ftp.cmdl.noaa.gov, *Dlugokencky et al.*, 1994, 2001] to define the latitudinal gradient of CH_4 concentrations at the surface. From this initial state with no vertical gradients in the troposphere, we conduct a 2-year spin-up simulation with 2000 meteorological fields and the *Wang et al.* [2003] emissions to construct the vertical and longitudinal gradients of CH_4. The results from this two-year spin-up are then scaled globally with a uniform factor to optimize agreement with the NOAA/CMDL surface data for December 2000.

Evaluation of the model background for the TRACE-P period is shown in figure 3 by comparison of model results for March 2001 with observations from NOAA/CMDL sites. The model reproduces the latitudinal gradient in the background without bias over the range of interest (10-50˚N), except at a few continental sites around 45˚N (LEF, HUN) where observed concentrations are high due to local source influence. Simulation of vertical gradients is discussed below using the TRACE-P observations.

3. *Model simulation of TRACE-P observations*

We first examine the ability of the model driven by a priori sources from the *Wang et al.* [2003] inventory (Table 1) to reproduce the general features of the CH_4 distributions and CH_4-C_2H_6-CO correlations observed in TRACE-P. The TRACE-P CH_4 measurements rely on the same calibration standards as NOAA/CMDL so that CH_4 concentrations should be consistent across the two data sets. We will show also results from a simulation where the *Streets et al.* [2003] anthropogenic emissions for CH_4 in East Asia have been superimposed on the *Wang et al.*

[2003] inventory. The ability of the model to simulate C_2H_6 observations using the sources in Table 2 will also be examined. A similar evaluation for CO, also using the sources of Table 2, was presented by *Palmer et al.* [2003a] and is not reported here. Throughout this paper, the model values are sampled along the flight tracks, and the observations are averaged over model grid boxes. Stratospheric data (O_3 > 100ppb with CO < 100ppb) are excluded. The observations are averaged over model grid boxes, corresponding to an averaging time span of 10-30 minutes for typically aircraft speeds. The model results are output every 3 hours. Considering that we are looking at aged air masses, at least one day downwind of the sources, the time discrepancy between the model and observation should be negligible. Linear regressions use the RMA (reduced major axis) method [*Hirsch and Gilroy,* 1984], accounting for errors in both variables.

3.1.   *Methane*

Figure 4a (top panel) compares the simulated and observed CH_4 concentrations for the ensemble of TRACE-P observations over the NW Pacific (west of 160˚E). The simulation shows strong correlation with observations (r^2=0.71). The 6% positive bias (slope of the RMA regression line) is driven by boundary layer Asian outflow rather than by the background. This structure in the bias is more apparent in Figure 4b, which shows the simulated vs. observed mean vertical gradients of CH_4 concentrations in TRACE-P west of 160˚E. Model results using the *Streets et al.* [2003] East Asian inventory are also shown. We distinguish between data north of 30˚N where anthropogenic outflow was strongest, and south of 30˚N where most of the Southeast Asian biomass burning influence was observed [*Palmer et al.,* 2003a]. The model results with *a priori* sources show positive bias in the simulation of the Asian outflow enhancement at 0-6 km altitude, particularly north of 30˚N. The bias is larger when the *Streets et al.* [2003] inventory is used due to higher livestock and landfill emissions in that inventory. Rice emissions are lower in the *Streets et al.* [2003] inventory than in *Wang et al.* [2003], resulting in total annual East Asian CH_4 emissions that are similar between the two inventories (Table 1). However, the rice emissions are at low latitudes (Figure 2) and are also at their seasonal minimum in February-April, thus making little contribution to the Asian outflow observed in

TRACE-P. Although it would seem from Figure 4b that the *Streets et al.* [2003] inventory degrades the simulation, we will show in section 4 that using that inventory in combination with a decrease in Eurasian emissions provides in fact a good fit to CH_4 concentrations for the TRACE-P period.

Figure 4c (left panel) compares simulated and observed CH_4 concentrations west of 160˚E as a function of latitude and at different altitudes. Also shown (dashed lines) is the contribution of the CH_4 background (emitted before January 1, 2001) to the model fields. The model reproduces the general increasing trend of CH_4 with latitude, reflecting both the background and the Asian outflow enhancements. The model underestimates observations south of 16˚N, but these are mainly from a single flight over the South China Sea (figure 1) which makes interpretation difficult. CH_4 enhancements above the background in the model fields (difference between solid and dashed lines) reflect emissions over the January-April 2001 period. As shown in Figure 4c (right panels), we find that East Asian sources contribute most of this enhancement south of 35˚N, while Eurasian sources (Europe and eastern Russia, the former is about 80%) dominate north of 35˚N. The principal East Asian sources contributing to the enhancements below 4 km are livestock, landfills, and coal mining. The principal Eurasian sources contributing to the Asian outflow are natural gas, landfills, and livestock. Biomass burning in Southeast Asia is a relatively large source south of 30˚N, mostly above 8 km (convective outflow), and at 2-4 km (WCB frontal outflow), consistent with TRACE-P observations for the HCN and CH_3CN biomass burning tracers [*Li et al.,* 2003*; Singh et al.,* 2003]. The wetlands source of CH_4 does not contribute significantly to the Asian outflow sampled in TRACE-P because it is located too far south (see Figure 2).

3.2.   Ethane

Comparisons of simulated and observed C_2H_6 concentrations are shown in Figure 5a (scatterplot), Figure 5b (vertical profiles) and Figure 5c (latitudinal gradients). There is strong correlation in the ensemble of data ($r^2 = 0.73$). The regression slope of 1.04 in the scatterplot (Figure 5a) is mainly driven by the underestimate of the background. The magnitude of the

enhancement in Asian outflow is well described as shown in Figure 5b. The latitudinal gradients are similar to those of CH_4, and there is no distinct bias in the model for any of the major features. The Eurasian fossil fuel source makes the largest contribution to the model fields at all altitudes north of 30˚N. East Asian sources make only a minor contribution north of 30˚N, but are relatively more important to the south, where the Eurasian influence is less.

3.3. CH_4 - C_2H_6 - CO correlations

We saw in section 3.1 that the model with a priori sources reproduces the general latitudinal and vertical distributions of CH_4 in TRACE-P but is too high in the lower tropospheric Asian outflow. We will now examine what additional insights can be obtained from the observed CH_4-C_2H_6-CO correlations. Observed pollution plumes with CO concentrations greater than 325 ppb on a 5-minute average basis (4% of the data in all) are removed from the correlation analysis because they would otherwise overly influence the least-square statistics. We employ the bootstrap method [*Venables and Ripley,* 1999] to calculate the standard deviations of the slopes of the regression lines.

Figure 6 compares the simulated and observed CH_4-C_2H_6-CO correlations for regional subsets of the TRACE-P data. The slopes of the regression lines and associated standard deviations are given in Table 3. We will use the CH_4-C_2H_6 and CH_4-CO correlations as constraints on CH_4 sources, and the C_2H_6-CO correlation to test the relative influence of East Asian and Eurasian sources. The region north of 30˚N and below 2 km ("Chinese outflow") sampled anthropogenic outflow but was largely devoid of biomass burning influence [*Liu et al.,* 2003a; *Palmer et al.,* 2003a; *Russo et al.,* 2003; *Singh et al.,* 2003]. The region south of 30˚N and below 2 km ("tropical Asian outflow") has more influence of sources from the tropical Asian region. In order to obtain independent information on Japanese/Korean sources, we use data from DC-8 flight 17 (31 March) which sampled a mix of Japanese and Korean influences but with relatively little Chinese influence [*Blake et al.,* 2003; *Suntharalingam et al.,* 2003]. Finally, we also examine the correlations in background air (east of 160˚E and 2-8 km altitude).

For Chinese outflow (Figure 6a and Table 3), the simulated CH_4/CO and C_2H_6/CO slopes are consistent with observations while the CH_4/C_2H_6 slope is significantly too low (39±1.1 vs. 43±1.2 ×10^{-3} molar). The CH_4 and C_2H_6 concentrations in Chinese outflow reflect contributions from anthropogenic sources in both East Asia and Eurasia (section 3.1 and 3.2). Correction of the CH_4/C_2H_6 bias will be discussed in section 4.

For tropical Asian outflow (Figure 6b), the observed CH_4/CO and C_2H_6/CO slopes are higher than for Chinese outflow (0.46 vs. 0.38 for CH_4/CO, 11 vs. 8.5 ×10^{-3} molar for C_2H_6/CO) while the CH_4/C_2H_6 slopes are similar (42 vs. 43). As shown by the tagged CH_4 simulation, tropical CH_4 sources from wetlands and biomass burning are of little importance and anthropogenic sources of CH_4 from East Asia and Eurasia remain dominant in this region. The model captures the regional differences in the CH_4/CO and C_2H_6/CO slopes. However, it overestimates the CH_4/C_2H_6 and CH_4/CO slopes significantly.

Compared to the Chinese and tropical Asian outflow, the Japanese/Korean plumes (Figure 6c) feature significantly higher CH_4/C_2H_6 slopes (45 vs. 42-43), CH_4/CO (0.65 vs. 0.38-0.46), and C_2H_6/CO (14 vs. 9-11 ×10^{-3} molar). These regional differences are due to CO emission controls and to low biofuel emissions (characterized by a low CH_4/C_2H_6 emission ratio). Again, the model captures this regional variation. It overestimates the CH_4/C_2H_6 slope, and underestimates the C_2H_6/CO slope, with no significant bias in the CH_4/CO slope (Table 3).

Figure 6d shows the CH_4-C_2H_6-CO correlations in background air masses east of 160˚E. The observed slopes are much higher (58 for CH_4/C_2H_6, 0.75 for CH_4/CO, and 13 ×10^{-3} molar for C_2H_6/CO) than in Asian outflow. These correlations reflect the common large-scale latitudinal gradients of the three gases. The model reproduces all these correlations without significant bias.

4.   *Optimization of CH$_4$ sources*

We have shown that both East Asian and Eurasian anthropogenic sources were major contributors to the CH_4 enhancement in Asian outflow observed in TRACE-P, and that the correlations of CH_4 with C_2H_6 and CO have distinct characteristics related to both regional

sources and background. We seek now to use the constraints from the observed CH_4 enhancements and CH_4-C_2H_6-CO correlations to optimize the representation of CH_4 sources in the model in a forward fashion. Considering that the C_2H_6 and CO simulations match the observations closely (see section 3.2 and *Palmer et al.* [2003]), we focus here on adjusting CH_4 emissions only. Since the East Asian and Eurasian anthropogenic sources are two dominant components affecting the structure of CH_4 Asian outflow during TRACE-P, we choose to fit the model to the observations by adjusting these two CH_4 emission variables. We do not try to resolve the individual anthropogenic source components of CH_4 within each region because of strong spatial source overlap (figure 2) which precludes detection of individual signatures in the outflow.

We focus on the data for Chinese outflow (Figure 6a), which provide the strongest regional constraints on sources and for which model transport errors are smallest because no vertical motions are involved [*Kiley et al.,* 2003]. The model with a priori sources overestimates the CH_4 enhancement in this data set by 7 ppb (Figure 4b). The observed CH_4/C_2H_6 and CH_4/CO slopes are 43 ± 1.2 mol mol^{-1} and 0.38 ± 0.02 mol mol^{-1}, respectively, while the corresponding model slopes are 39 ± 1.1 mol mol^{-1} and 0.38 ± 0.02 mol mol^{-1} (Table 3). We seek to satisfy the observed CH_4 enhancements, and the observed CH_4/C_2H_6 and CH_4/CO correlations, by adjusting CH_4 anthropogenic sources from East Asia and Eurasia in the model. Figure 7 shows the simulated CH_4/C_2H_6 and CH_4/CO slopes, and the difference between simulated and observed mean CH_4 concentration enhancements in the Chinese boundary layer outflow, as a function of percentage changes in these two emission variables relative to the a priori. We aim to fit the observed mean CH_4 enhancements to within 5 ppb and the slopes to within the 95% confidence interval from the bootstrap method ($\pm1.96\sigma$), i.e., 40-46 for CH_4/C_2H_6 and 0.34-0.42 for CH_4/CO. These ranges are shown as green and black lines in Figure 7. The domain of model space satisfying the three constraints is shaded in Figure 7. It defines our range of optimized East Asian and Eurasian anthropogenic emissions.

The model simulation with a priori sources is represented by point A in Figure 7. The positive model bias in simulating the CH_4 concentration enhancement in Asian outflow could be

caused by an overestimate of either East Asian or Eurasian sources. We see from Figure 7 that simply decreasing either of these (or both) would cause the CH_4/C_2H_6 slope to be too low. Fitting the CH_4/C_2H_6 constraint requires an increase in East Asian emissions, and thus our solution involves increasing the East Asian and decreasing the Eurasian anthropogenic emissions both by at least 30% (point C).

A 40% increase in springtime East Asian anthropogenic emissions relative to the a priori *Wang et al.* [2003] inventory can be achieved simply by using instead the emission inventory of *Streets et al.* [2003] (Table 1). Although that inventory is comparable to *Wang et al.* [2003] on an annual basis, it is 40% higher in March-April when the rice paddy source is at its seasonal minimum, as discussed in section 2. Such a 40% increase of East Asian sources requires from Figure 7 a corresponding decrease in Eurasian sources of 30-50%.

Table 3 gives the simulated CH_4/C_2H_6 and CH_4/CO slopes in the different TRACE-P regional data subsets for (1) the a priori simulation; (2) the a priori but with *Streets et al.* [2003] East Asian anthropogenic sources; (3) the a priori but with Eurasian anthropogenic sources decreased by 30-50%; (4) the combination of (2) and (3). Using the *Streets et al.* [2003] emission inventory increases the CH_4/C_2H_6 and CH_4/CO slopes in Chinese outflow, while decreasing the Eurasian sources decreases the slopes. Results with our optimized (4) emissions indicate a general improvement in the simulation of the observed correlations for the tropical Asian as well as the Chinese boundary layer outflow, while there is little effect on the Japanese/Korean and background data subsets. The effects on the simulations of the CH_4 vertical profiles and the CH_4-C_2H_6-CO correlations are shown in Figures 4 and 6. The ability of the model to fit the observations is clearly improved; only the CH_4/CO slopes in the Chinese outflow and Japanese/Korean outflow are slightly worse. With the optimized CH_4 sources, the simulated CH_4 concentrations in March 2001 at CMDL surface sites north of 30°N are 7 ppb lower on average than with the a priori simulation (Figure 3), while there is little difference south of 30°N.

Our a priori total of 68 Tg yr^{-1} for the Eurasian anthropogenic source from *Wang et al.* [2003], is comparable to that in the EDGAR3.2 [*Olivier,* 2001a] bottom-up inventory (64 Tg yr^{-1}). These inventories were constructed for the years 1998 and 1995 respectively. Aside from the

intrinsic uncertainties in emission estimates, it is also likely that Eurasian emissions have decreased in recent years due to increased mitigation efforts. Such mitigation efforts involve, for example, capture and utilization of CH_4 from landfills and coal mining, and a shift from underground to surface mining of coal [*Olivier*, 2002; EPA, 2001]. Our results suggest that large decreases in Eurasian emissions of CH_4 could have taken place over the past decade.

5.   *Conclusions*

Large CH_4 enhancements above background were observed in Asian outflow over the NW Pacific during the TRACE-P aircraft mission (March-April, 2001). The CH_4 enhancements showed strong correlations with C_2H_6 and CO that varied with the outflow region. We used a global chemical transport model (GEOS-CHEM) simulation of the CH_4-C_2H_6-CO system for the TRACE-P period to interpret these observations with the goal of better quantifying CH_4 regional sources.

Our a priori model simulation uses the *Wang et al.* [2003] global CH_4 emission inventory previously derived from inverse modeling of NOAA/CMDL observations. It reproduces the general latitudinal and vertical distributions of CH_4 observed during TRACE-P, but overestimates by about 7 ppb the CH_4 enhancement in Asian outflow. This enhancement is driven by anthropogenic sources in both East Asia and Eurasia (defined here as Europe + eastern Russia). The a priori model also underestimates the CH_4/C_2H_6 slopes in Chinese outflow, and overestimates them in tropical Asian outflow and in Japanese/Korean plumes. It reproduces the observed CH_4/CO slopes without significant bias except for an overestimate in tropical Asian outflow. We find that the CH_4-C_2H_6-CO correlations in the Asian outflow observed in TRACE-P are defined mainly by anthropogenic sources of CH_4 (landfills, livestock and fossil fuel) from East Asia and Eurasia, rather than by biomass burning or wetland sources from tropical Southeast Asia. Emissions from rice cultivation did not make a significant contribution to the CH_4 outflow in TRACE-P, in part because they are at low latitudes and in part because they were at their seasonal minimum during the TRACE-P period. Observations in late summer or early fall would be expected to see a stronger influence from rice cultivation CH_4 emissions.

We employ the constraints offered by the observed CH_4 enhancements and the CH_4-C_2H_6-CO correlations to optimize our estimates of the CH_4 anthropogenic emissions in East Asia and Eurasia. To correct the positive model bias of CH_4 concentrations in the boundary layer Chinese outflow while increasing the CH_4/C_2H_6 slope and maintaining the CH_4/CO slope, we find that we need to increase the East Asian and decrease the Eurasian anthropogenic sources of CH_4 by at least 30% for both. The increase in East Asian emissions is imposed by the constraint on the CH_4/C_2H_6 slope. Without this increase, the model slope would be too low.

A 40% increase in East Asian anthropogenic emissions for the TRACE-P period relative to the *Wang et al.* [2003] inventory can be implemented simply by substituting the *Streets et al.* [2003] regional inventory for East Asia prepared in support of the TRACE-P mission. The *Streets et al.* [2003] inventory has higher livestock and landfill emissions. The Eurasian anthropogenic source (80% European) then needs to be reduced by 30-50% from the *Wang et al.* [2003] inventory. Decrease of European CH_4 emissions could have taken place over the past decade due to mitigation efforts. Intrinsic uncertainties in the a priori emission inventory must also be considered.

We have shown in this work that observed CH_4-C_2H_6-CO correlations in continental outflow place valuable constraints on the CH_4 budget. In our application, these constraints allowed us to distinguish between East Asian and Eurasian source signatures in Asian outflow over the Pacific, and to conclude that the overestimate of CH_4 in our simulation with a priori sources had to be corrected by both decreasing the Eurasian source and (remarkably) increasing the East Asian source. A more formal inverse modeling approach for the CH_4-C_2H_6-CO system should be applied in a next stage to better exploit the constraints from the correlations. Improved understanding of C_2H_6 sources (adjusted here in a top-down fashion to match observations) will be needed in order to better relate CH_4-C_2H_6 correlations to the fossil fuel source of CH_4.

References

Andreae M. O., P. Merlet P, Emission of trace gases and aerosols from biomass burning, *Global Biogeochemical Cycles,* 15 (4): 955-966, 2001.

Bartlett K. B., G. W. Sachse, J. E. Collins, R. C. Harriss, Methane in the tropical South Atlantic: Sources and distribution during the late dry season, *J. Geophys. Res.*, 101 (D19): 24139-24150, 1996.

Bartlett K. B., G. W. Sachse, T. Slate, C. Harward, D. B. Blake, Large-scale distribution of CH4 in the western North Pacific: Sources and transport from the Asian continent, *J. Geophys. Res.*, *108(D20):* Art. No. 8807, 2003.

Bertschi, I. T., R. J. Yokelson, D. E. Ward, T. J. Christian, and W. M. Hao, Trace gas emissions from the production and use of domestic biofuels in Zambia measured by open-path Fourier transform infrared spectroscopy, *J. Geophys. Res.*, *108*(D13), 8469, doi:10.1029/2002JD002158, 2003.

Bey, I., et al., Global modeling of tropospheric chemistry with assimilated meteorology: Model description and evaluation, *J. Geophys. Res.*, *106*, 23,073–23,096, 2001a.

Bey, I., D. J. Jacob, J. A. Logan, and R. M. Yantosca, Asian chemical outflow to the Pacific: origins, pathways and budgets, *J. Geophys. Res.*, *106*, 23,097–23,114, 2001b.

Blake D. R., F. S. Rowland, Global atmospheric concentrations and sources strength of ethane, *Nature,* 321 (6067): 231-233, 1986.

Blake, N. J., D. R. Blake, B. C. Sive, T.-Y. Chen, F. S. Rowland, J. E. Collins Jr., G. W. Sachse, and B. E. Anderson, Biomass burning emissions and vertical distribution of atmospheric methyl halides and other reduced carbon gases in the South Atlantic region, *J. Geophys. Res.*, *101*, 24,151–25,164, 1996.

Blake, N. J., et al., NMHCs and halocarbons in Asian continental outflow during TRACE-P: Comparison to PEM-West B, *J. Geophys. Res.*, *108*(D20), 8806, doi:10.1029/2002JD003367, 2003.

Boissard C., B. Bonsang, M. Kanakidou, G. Lambert, TROPOZ II: Global distributions and budgets of methane and light hydrocarbons, *J. Atmos. Chem.,* 25, 115-148, 1996.

Cicerone, R.J., and R.S. Oremland, Biogeochemical aspects of atmospheric methane, *Global Biogeochemical Cycles, 2,* 299-327, 1988.

DeMore, W. B. et al., Chemical kinetics and photochemical data for use in stratospheric modeling, *JPL Publ. 97-4,* 1997.

Dlugokencky, E. J., L. P. Steele, P. M. Lang, and K. A. Masarie, The growth rate and distribution of atmospheric methane, *J. Geophys. Res.*, *99*, 17,021–17,043, 1994.

Dlugokencky, E. J., K. A. Masarie, P. M. Lang, and P. P. Tans, Continuing decline in the growth rate of the atmospheric methane burden, *Nature*, *393*, 447–450, 1998.

Dlugokencky, E. J., B. P. Walter, K. A. Masarie, P. M. Lang, and E. S. Kasischke, Measurements of an anomalous global methane increase during 1998, *Geophys. Res. Lett., 28*, 499-502, 2001.

Duncan, B. N., R. V. Martin, A. C. Staudt, R. Yevich, J. A. Logan, Interannual and Seasonal Variability of Biomass Burning Emissions Constrained by Satellite Observations, *J. Geophys. Res., 108(D2)*), 4040, doi:10.1029/2002JD002378, 2003a.

Duncan, B.N., J. A. Logan, I. Bey, R. V. Martin, D. J. Jacob, R. M. Yantosca, P. C. Novelli, N. B., Jones, C. P. Rinsland, Model study of the variability and trends of carbon monoxide (1988-1997): 1, Model formulation, evaluation, and sensitivity, 2. Trends and regulating factors, *J. Geophys. Res.,* submitted, 2003b.

EPA, Non-CO2 Greenhouse Gas Emissions from Developed Countries: 1990-2010, Report No. EPA-430-R-01-007, U.S. Environmental Protection Agency, Washington, D.C., 2001.

Etheridge, D. M., L. P. Steele, R. J. Francey, R. L. Langenfelds, Atmospheric methane between 1000 AD and present: Evidence of anthropogenic emissions and climatic variability, *J. Geophys. Res.*, *103*, 15,979-15,993, 1998.

Flores R. M., J. H. Chen, V. G. Mcdonell and G. S. Samuelsen, Effect of natural gas composition on the performance of a model gas turbine combustor, Combustion laboratory, ATS Annual workshop, Pittsurgh, PA 8-10 Nov 1999.

Fiore, A. M., D. J. Jacob, I. Bey, R. M. Yantosca, B. D. Field, and J. Wilkinson, Background ozone over the United States in summer: origin and contribution to pollution episodes, *J. Geophys. Res.*, *107(D15):* Art. No. 4275, 2002.

Fiore, A. M., D. J. Jacob, H. Liu, R. M. Yantosca, T. D. Fairlie, and Q. Li, Variability in surface ozone background over the United States: Implications for air quality policy, *J. Geophys. Res., 108,* 4787, doi:10.1029/2003JD003855, 2003.

Fuelberg, H. E., C. M. Kiley, J. R. Hannan, D. J. Westberg, M. A. Avery, and R. E. Newell, Atmospheric transport during the Transport and Chemical Evolution over the Pacific (TRACE-P) experiment, *J. Geophys. Res., 108 (D20):* Art. No. 8782, 2003.

Fung, I., J.John, J. Lerner, E. Matthews, M. Prather, L.P. Steele, and P.J. Fraser, Three-dimensional model synthesis of the global methane cycle, *J. Geophysical Research, 96*, 13,033- 13,065, 1991.

Gupta M., S. Tyler S, R. Cicerone, Modeling atmospheric $\delta^{13}CH_4$ and the causes of recent changes in atmospheric CH_4 amounts, *J. Geophys. Res., 101(D17),* 22923-22932, 1996.

Gupta M. L., R. J. Cicerone, D. R. Blake, F. S. Rowland, I.S.A. Isaksen, Global atmospheric distributions and source strengths of light hydrocarbons and tetrachloroethene, *J.Geophy.Res.,* 103, 28219-28235, 1998.

Hansen, J., M. Sato, R. Ruedy, A. Lacis, and V. Oinas, Global warming in the twenty-first century: An alternative scenario, *Proc. Natl. Acad. Sci., USA, 97*, 9875-9880, 2000.

Harriss, R. C., G. W. Sachse, J. E. Collins Jr., L. Wade, K. B. Bartlett, R. W. Talbot, E. V. Browell, L. A. Barrie, G. F. Hill, and L. G. Burney, Carbon monoxide and methane over Canada: July–August 1990, *J. Geophys. Res.*, *99*, 1659–1669, 1994.

Heald, C. L., D. J. Jacob, P. I. Palmer, M. Evans, G. Sachse, D. Blake, and H. Singh, Biomass burning emission inventory with daily resolution: Application to aircraft observations of Asian outflow, *J. Geophys. Res.*, *108*(D21), 8811, doi:10.1029/2002JD003082, 2003a.

Heald, C.L., D.J. Jacob, L. Emmons, J.C. Gille, G.W. Sachse, E.V. Browell, M.A. Avery, and S.A. Vay, Transpacific transport and chemical evolution of Asian pollution observed from satellite and aircraft, *J. Geophys. Res.,* in press, 2003b.

Hein, R., P.J. Crutzen, and M. Heimann, An inverse modeling approach to investigate the global atmospheric methane cycle, *Global Biogeochemical Cycles,* 11, 43-76, 1997.

Hirsch R. M., E. J. Gilroy, Methods of fitting a straight line to data: examples in water resources, *Water Resources Bulletin,* 20(5), 1984.

Houweling, S., T. Kaminski, F. Dentener, J. Lelieveld, and M. Heimann, Inverse modeling of methane sources using the adjoint of a global transport model, *J. Geophys. Res., 104*, 26,137-16,160, 1999.

IPCC, Intergovernmental Panel on Climate Change, United Nations Environment Programme, Organization for Economic Co-operation and Development, International Energy Agency, 2001.

Jacob, D. J., J. H. Crawford, M. M. Kleb, V. S. Connors, R. J. Bendura, J. L. Raper, G. W. Sachse, J. C. Gille, L. Emmons, and C. L. Heald, The Transport and Chemical Evolution over the Pacific (TRACE-P) aircraft mission: design, execution, and first results, *J. Geophys. Res., 108* (D20): 1-19, 2003.

Jaeglé, L., D. Jaffe, H. U. Price, P. Weiss, P. I. Palmer, M. J. Evans, D. J. Jacob, and I. Bey, Sources and budgets for CO and O_3 in the northeastern Pacific during the spring of 2001: results from the PHOBEA-II experiment, *J. Geophys. Res., 108,* 8803, doi:10.1020/2002JD003121, 2003.

Kanakidou M., H. B. Singh, K. M. Valentin, P. J. Crutzen, A two-dimensional study of ethane and propane oxidation in the troposphere, *J. Geophys. Res.,* 96, 15395-15413, 1991.

Kiley, C. M., H. E. Fuelberg, P. I. Palmer, D. J. Allen, G. R. Carmichael, D. J. Jacob, C. Mari, R. B. Pierce, K. E. Pickering, Y. Tang, O. Wild, T. D. Fairlie, J. A. Logan, G. W. Sachse, T. K. Shaack, D. G. Streets, An intercomparison and evaluation of aircraft‐derived and simulated CO from seven chemical transport models during the TRACE‐P experiment, *J. Geophys. Res.,*108, 8819, doi:10.1029/2002JD003089, 2003.

Lerner, J., E. Matthews and I. Fung, Methane emission from animals: a global high resolution data base, *Global Biogeo. Cycles, 2*, 139-156, 1988.

Li, Q., D. J. Jacob, R. M. Yantosca, C. L. Heald, H. B. Singh, M. Koike, Y. Zhao, G. W. Sachse, and D. G. Streets, A global 3-D model evaluation of the atmospheric budgets of HCN and CH3CN: constraints from aircraft measurements over the western Pacific, *J. Geophys. Res.,* 108(D21), 8827, doi:10.1029/2002JD003075, 2003.

Liu, H., D. J. Jacob, I. Bey, R. M. Yantosca, B. N. Duncan, and G. W. Sachse, Transport pathways for Asian combustion outflow over the Pacific: interannual and seasonal variations, *J. Geophys. Res., 108 (D20),* 8786, doi:10.1029/2002JD003102, 2003a.

Liu, H., D. J. Jacob, J. E. Dibb, A. M. Fiore, and R. M. Yantosca, Constraints on the sources of tropospheric ozone from ^{210}Pb-^{7}Be-O$_3$ correlations, *J. Geophys. Res.,* in press, 2003b.

Lowe D. C., C. Brenninkmeijer, S. C. Tyler, E. J. Dlugkencky, Determination of the isotopic composition of atmospheric methane and its application in the Antarctic, *J. Geophys. Res., 96(D8),* 15455-15467, 1991.

Lowe D. C., C. Brenninkmeijer, G. W. Brailsford, K. R. Lassey, A. J. Gomez, E. G. Nisbet, Concentration and C13 records of atmospheric methane in New Zealand and Antarctic – Evidence for changes in methane sources, *J. Geophys. Res., 99(D8),* 16913-16925, 1994.

Matsueda H., H. Y. Inoue, Aircraft measurements of trace gases between Japan and Singapore in October of 1993, 1996, and 1997, *Geophys. Res.Lett.*, 26 (16): 2413-2416, 1999.

Matthews, E., and I. Fung. Methane Emissions from Natural Wetlands: Global Distribution, Area, and Ecology of Sources, *Global Biogeochemical Cycles, 1,* 61-86, 1987.

Matthews, E., I. Fung, and J. Lerner, Methane emissions from rice cultivation: geographic and seasonal distribution of cultivated areas and emissions, *Global Biogeochemical Cycles, 5*, 3-24, 1991.

Mikaloff Fletcher, S.E., P.P. Tans, L.M. Bruhwiler, J.B. Miller, and M. Heimann, Constraining CH$_4$ source estimates with atmospheric Observations of CH$_4$ and its ^{13}C/^{12}C isotopic ratios in CH$_4$: Part 1. Inverse modeling of source processes, Global Biogeochem. Cycles, in revision, 2004.

Mikaloff Fletcher, S.E., P.P. Tans, L.M. Bruhwiler, J.B. Miller, and M. Heimann, Constraining CH$_4$ source estimates with atmospheric Observations of CH$_4$ and its ^{13}C/^{12}C isotopic ratios in CH$_4$: Part 2. Inverse modeling of fluxes from geographical regions, Global Biogeochem. Cycles, in revision, 2004.

Miller J. B., K. A. Mack, R. Dissly, J. W. C White, E. J. Dlugokencky, P. P. Tans, Development of analytical methods and measurements of C-13/C-12 in atmospheric CH$_4$ from the NOAA Climate Monitoring and Diagnostics Laboratory global air sampling network, *J. Geophys. Res., 107 (D13)*: Art. No. 4178, 2002.

Olivier, J.G.J. and J.J.M. Berdowski. (2001a) Global emissions sources and sinks. In: Berdowski, J., Guicherit, R. and B.J. Heij (eds.) "The Climate System", pp. 33-78. A.A. Balkema Publishers/Swets & Zeitlinger Publishers, Lisse, The Netherlands. ISBN 90-5809-255-0.

Olivier, J.G.J. (2002) Greenhouse gas emissions: 1. Shares and trends in greenhouse gas emissions; 2. Sources and Methods. In: "CO$_2$ emissions from fuel combustion 1971-2000", 2002 Edition, pp. III.1-III.31. International Energy Agency (IEA), Paris. ISBN 92-64-09794-5.

Palmer, P. I., D. J. Jacob, D. B. Jones, C. L. Heald, R. M. Yantosca, J. A. Logan, G. W. Sachse, and D. G. Streets, Inverting for emissions of carbon monoxide from Asia using aircraft observations over the western Pacific, *J. Geophys. Res., 108,* 8828, doi:10.1029/2003JD003397, 2003a.

Palmer, P. I., D. J. Jacob, L. J. Mickley, D. R. Blake, G. W. Sachse, H. E. Fuelberg, and C. M. Kiley, Eastern Asian emissions of anthropogenic halocarbons deduced from aircraft concentration data, *J. Geophys. Res., 108,* 4753, doi:10.1029/2003JD003591, 2003b.

Prinn, R. G., R. F. Weiss, B. R. Miller, J. Huang, F. N. Alyea, D. M. Cunnold, P. J. Fraser, D. E. Hartley, P. G. Simmonds, Atmospheric trends and lifetime of CH_3CCl_3 and global OH concentrations, *Science,* 269 (5221): 187-192, 1995.

Prinn, R. G. et al., Evidence for substantial variations of atmospheric hydroxyl radical in the past two decades, *Science, 292,* 1882-1997, 2001.

Quay P., J. Stutsman, D. Wilbur, A. Snover, E. Dlugokencky, T. Brown, The isotopic composition of atmospheric methane, *Global Biogeochemical Cycles,* 13 (2): 445-461, 1999.

Rudolph J., The tropospheric distribution and budget of ethane, *J.Geophys. Res.,* 100, D6, 11369-11381, 1995.

Russo R. S., R. W.Talbot, J. E. Dibb, E. Scheuer, G. Seid, C. E. Jordan, H. E. Fuelberg, G. W. Sachse, M.A. Avery, S. A. Vay, D. R. Blake, N. J. Blake, E. Atlas, A. Fried, S. T. Sandholm, D. Tan, H. B. Singh, J. Snow, B. G. Heikes, Chemical composition of Asian continental outflow over the western Pacific: Results from Transport and Chemical Evolution over the Pacific (TRACE-P), *J.Geophys. Res.,* 108 (D20): Art. No. 8804, 2003.

Shipham M. C., P. M. Crill, K. B. Bartlett, A. H. Goldstein, P. M. Czepiel, R. C. Harriss, D. Blaha, Methane measurements in central New England: An assessment of regional transport from surrounding sources, *J.Geophys. Res.,* 103 (D17): 21985-22000, 1998.

Singh H. B., A. Tabazadeh, M. J. Evans, B. D. Field, D. J. Jacob, G. W. Sachse, J. H. Crawford, R. Shetter, W. H. Brune, Oxygenated volatile organic chemicals in the oceans: Inferences and implications based on atmospheric observations and air-sea exchange models, *J. Geophys. Letter,* 30, 1862, doi:10.1029/2003GL017933, 2003.

Spivakovsky, C. M., J. A. Logan, S. A. Montzka, Y. J. Balkanski, M. Foremen-Fowler, D. B. A. Jones, L. W. Horowitz, C. A. M. Brenninkmeijer, M. J. Prather, S. C. Wofsy, and M. B. McElroy, Three dimensional climatological distribution of tropospheric OH: update and evaluation, *J. Geophys. Res., 105,* 8931-8980, 2000.

Staudt, A. C., D. J. Jacob, F. Ravetta, J. A. Logan, D. Bachiochi, T. N. Krishnamurti, S. Sandholm, B. Ridley, H. B. Singh, B. Talbot, Sources and chemistry of nitrogen oxides over the tropical Pacific, *J. Geophys. Res.,* 108(D2), 8239, doi:10.1029/2002JD002139, 2003.

Streets, D.G., T. C. Bond, G. R. Carmichael, S. D. Fernandes, Q. Fu, D. He, Z. Klimont, S. M. Nelson, N. Y. Tsai, M. Q. Wang, J.-H. Woo, and K. F. Yarber, An inventory of gaseous and primary aerosol emissions in Asia in the year 2000, *J. Geophys. Res., 108 (D21),* 8809, doi:10.1029/2002JD003093, 2003.

Suntharalingam P., D. Jacob, P. Palmer, J. Logan, Y. Xiao, R. Yantosca, D. Streets, S. Vay and G. Sachse, Improved Quantification of Chinese Carbon Fluxes Using CO_2/CO Correlations in Asian Outflow, *J. Geophys. Res.,* submitted, 2003.

Venables W. N. and B.D. Ripley, Modern Applied Statistics with S-PLUS. Third Edition, Springer. ISBN 0-387-98825-4, 1999.

Wang Y. H., D. J. Jacob, J. A. Logan, Global simulation of tropospheric O_3-NOx-hydrocarbon chemistry: 1. Model formulation, *J.Geophys. Res.,* 103, 10713-10725, 1998.

Wang, J. S., J. A. Logan, M. B. McElroy, B. N. Duncan, I. A. Megretskaia, and R. M. Yantosca, A 3-D model analysis of the slowdown and interannual variability in the methane growth rate from 1988 to 1997, *Global Biogeochemical Cycles,* submitted, 2003.

Yokelson R. J., I. T. Bertschi, T. J. Christian, P. V. Hobbs, D. E. Ward, W. M. Hao, Trace gas measurements in nascent, aged, and cloud-processed smoke from African savanna fires by airborne Fourier transform infrared spectroscopy (AFTIR), *J. Geophys. Res.,* 108 (D13): Art. No. 8478, 2003.

Yevich, R. and J. A. Logan, An assesment of biofuel use and burning of agricultural waste in the developing world, *Global Biogeochem. Cycles*, 17 (4), 1095, doi:10.1029/2002GB001952, 2003.

Table 1. East Asian[a] and Global CH$_4$ emissions (Tg yr^{-1})

	Wang et al. [2003][b]		Streets et al. [2003][c]	Olivier [2001a] (EDGAR3.2)[c]	
Year	1998		2000	1995	
	East Asia[d]	Globe	East Asia	East Asia	Globe
Total anthropogenic	113	286	106	117	284
Rice cultivation	52(40%)	59	24	36	39
Livestock	27	83	36	28	89
Fossil fuel					
Coal mining	14	31	8	14	33
Gas/oil	4.8	52	5.8	6.6	53
Landfills	9.7	50	23	21	56
Biofuel	5.8	9.2	8.6	8.3	14
Total natural	45	231	-	-	-
Biomass burning	4.3(240%)	21	3.1	1.8	13
Wetlands	36(80%)	185	-	-	-
Termites	4.6	25	-	-	-

[a]Including India (see figure 1).
[b]Used as a priori in this work.
[c]These inventories include only anthropogenic sources and biomass burning.
[d]Percentages in parentheses are the seasonal scaling factors for February-April 2001 (TRACE-P period) relative to the annual mean. For example, the value of 40% for rice cultivation means that the emissions in February-April are only 40% of the annual mean value.

Table 2. CH$_4$- C$_2$H$_6$ -CO emissions and emission ratios for Feb.-Apr. 2001[a]

	Global			East Asia[b]				Eurasia[c]	
	Fossil fuel	Biofuels	Biomass burning	Fossil fuel	Biofuels	Biomass burning	All anthropogenic sources[d]	Fossil fuel	All anthropogenic sources[d]
CH$_4$ (Tg)	21	2.3	6.8	3.6	0.93	0.95	12	7.7	15
C$_2$H$_6$ (Tg)	2.1	0.51	0.62	0.17	0.18	0.051	0.35	0.72	0.79
CO (Tg)	80	42	110	21	16	13.4	37	22	27
CH$_4$/C$_2$H$_6$ (molar)	19	8.5	20	40	10	35	64	20	37
CH$_4$/CO (molar)	0.46	0.10	0.11	0.30	0.10	0.12	0.57	0.62	1.0
C$_2$H$_6$/CO(10^{-3}molar)	25	11	5.3	7.6	10	3.6	8.8	31	27

[a]Total emissions for the 3-month period. CH$_4$ emissions are from *Wang et al.* [2003] (section 2.2.1) and are used here as our a priori. C$_2$H$_6$ sources are as described in section 2.2.2. CO emissions are from *Palmer et al.* [2003] (section 2.2.3). Emission ratios are calculated from the emission totals in the table.
[b]Excluding India.
[c]Including Europe and eastern Russia (see figure 1).
[d]Including contributions from rice cultivation, livestock, fossil fuel, landfill, and biofuel emissions.

Table 3. Slopes of CH_4-C_2H_6-CO relationships in Asian outflow over the NW Pacific (March-April 2001)[a]

		Chinese outflow (>30˚N, 0-2km)	Tropical Asian outflow (20-30˚N, 0-2km)	Japanese/Korean outflow	Background (2-8km, east of 160˚E)
TRACE-P Observations	CH_4/C_2H_6	43 ± 1.2	42 ± 1.7	45 ± 1.6	58 ± 2.2
	CH_4/CO	0.38 ± 0.02	0.46 ± 0.02	0.65 ± 0.03	0.75 ± 0.04
	C_2H_6/CO	8.5 ± 0.5	10.9 ± 0.5	14.4 ± 0.6	12.8 ± 0.7
GEOS-CHEM[b]					
(1) A priori [Wang et al., 2003]	CH_4/C_2H_6	39 ± 1.1	51 ± 0.9	54 ± 1.9	62 ± 1.3
	CH_4/CO	0.38 ± 0.02	0.60 ± 0.02	0.61 ± 0.04	0.84 ± 0.05
	C_2H_6/CO	10.0 ± 0.4	11.5 ± 0.4	11.3 ± 0.6	14.9 ± 0.9
(2) A priori with Streets et al. [2003] anthropogenic East Asian emissions[c]	CH_4/C_2H_6	47 ±1.7	52 ±1.2	59 ±2.8	64 ±1.2
	CH_4/CO	0.45 ±0.02	0.61 ±0.03	0.67 ±0.06	0.95 ±0.05
(3) A priori with Eurasian sources reduced by 30-50%[d]	CH_4/C_2H_6	33-35	44-47	45-49	55-57
	CH_4/CO	0.32-0.34	0.50-0.54	0.51-0.55	0.82-0.86
(4) Optimized; (2) and (3) combined[d]	CH_4/C_2H_6	41-43	43-46	50-54	57-59
	CH_4/CO	0.40-0.41	0.50-0.54	0.57-0.61	0.85-0.88

[a]Slopes of the reduced-major-axis (RMA) regressions for the regional subsets of data shown in Figure 6, with standard deviations computed by the bootstrap method (see text). Units are mol/mol for CH_4/C_2H_6 and CH_4/CO, 10^{-3} mol/mol for C_2H_6/CO.
[b]Results shown for simulations with different CH_4 sources. For all scenarios the CO simulation is from *Palmer et al.* [2003], in which Asian CO sources have been optimized through inversion analysis of the TRACE-P data; and C_2H_6 sources are as described in section 2.2.2.
[c]Superseding the corresponding *Wang et al.* [2003] sources in East Asia (Table 1).
[d]Slopes are given as ranges, with the low and high ends corresponding to Eurasian anthropogenic emission reductions of 50% and 30% respectively.
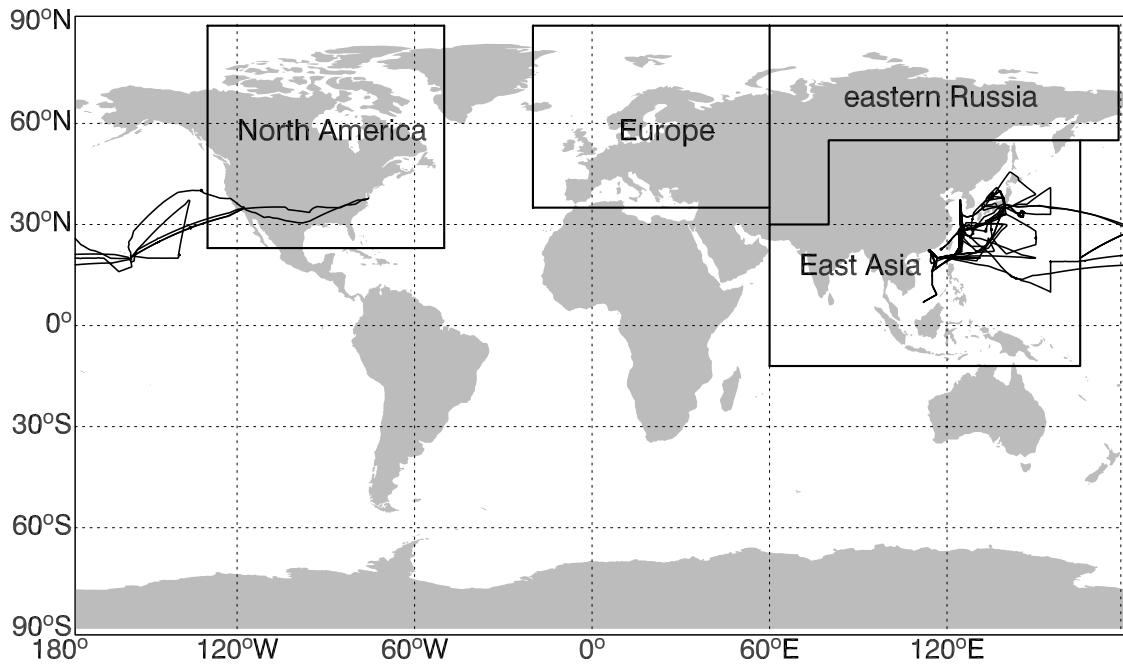
Figure 1. Tagged source regions for the CH$_4$, C$_2$H$_6$, and CO simulations. "Eurasia" in the text refers to the combination of Europe and eastern Russia. The TRACE-P flight tracks are also shown.
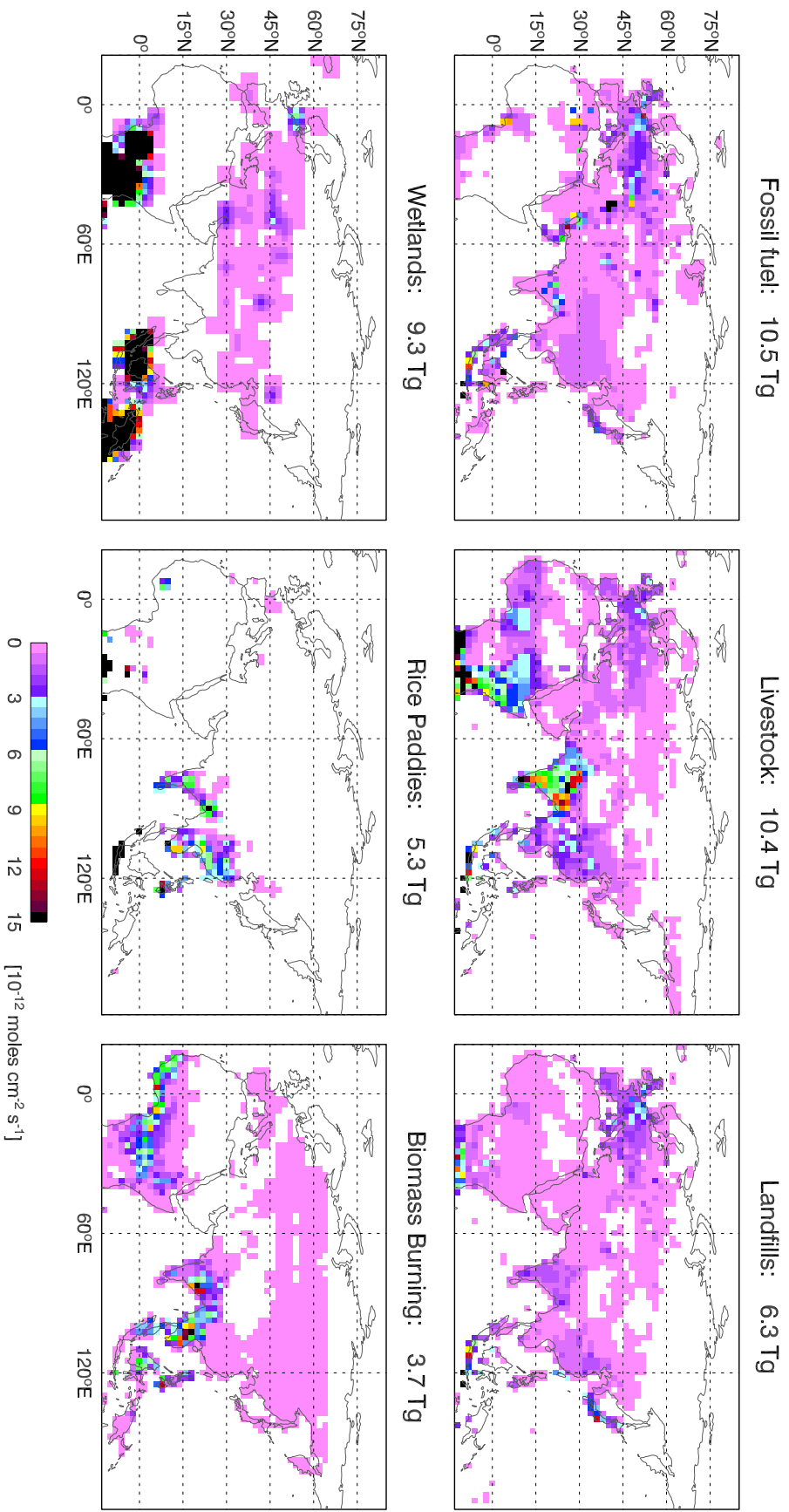
Figure 2. Distribution of CH$_4$ sources for the TRACE-P period (Feb.-Apr. 2001) based on Wang et al. [*2003*] and used as a priori in this work. Total emissions from East Asian and Eurasian sources over the 3-month period are indicated for each source on the top of the corresponding panel.
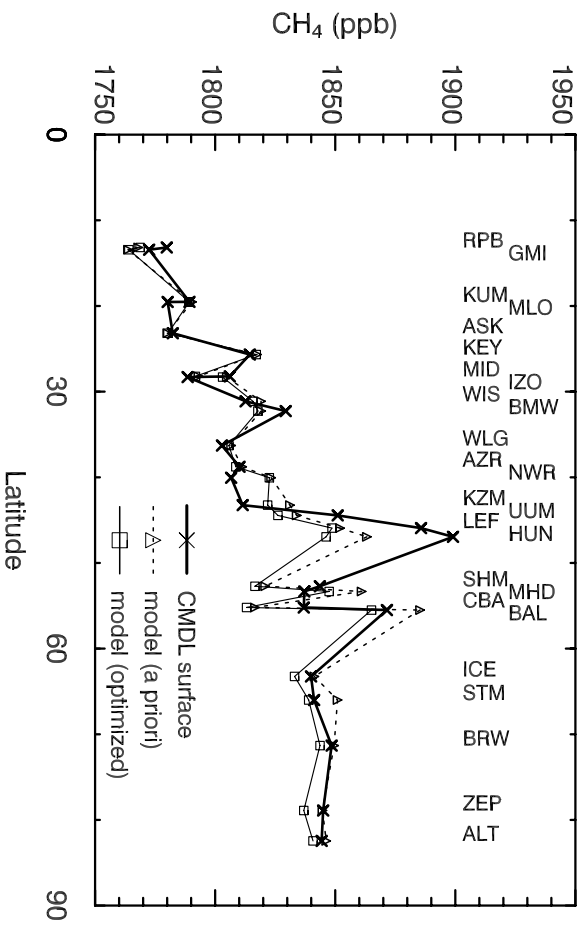
Figure 3. Simulated vs. observed latitudinal gradient of monthly mean CH_4 surface concentrations in March 2001 at the NOAA/CMDL surface sites north of 10°N [ftp://ftp.cmdl.noaa.gov]. The CMDL station code is displayed. Observations (bold solid line with crosses) are compared to model values using the a priori (dotted line with triangles) and optimized (solid line with squares) emission inventories. The a priori emission inventory is from *Wang et al.* [2003]. The optimized emission inventory fit to the TRACE-P data uses regional anthropogenic emissions from *Streets et al.* [2003] for East Asia and Eurasian anthropogenic emissions reduced by 50% from the *Wang et al.* [2003] inventory.
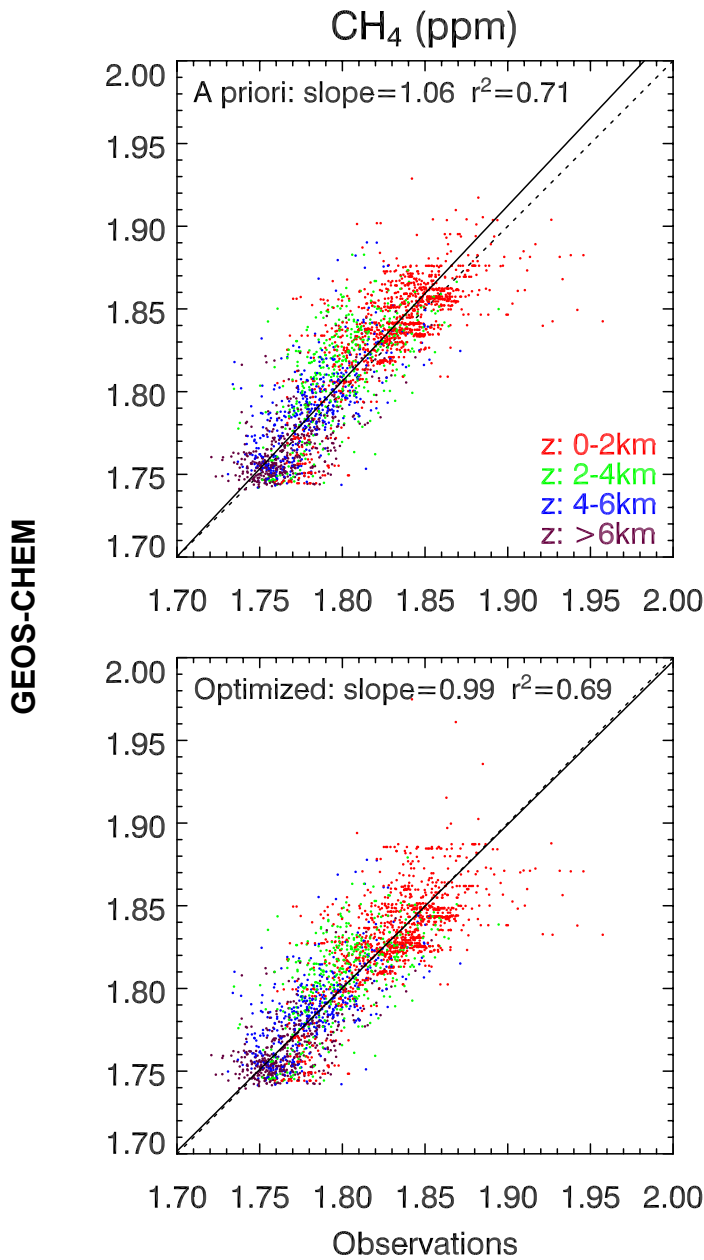
Figure 4a. Simulated vs. observed concentrations of CH_4 along the TRACE-P flight tracks over the northwest Pacific (west of 160˚E). Model results are shown for simulations with a priori (upper panel) and optimized (lower) emission inventories for CH_4. The model is sampled along the flight tracks, and the observations are averaged over the model grid boxes. The 1:1 line is shown as dotted. The solid line is the RMA regression line. The a priori emission inventory is from *Wang et al.* [2003]. The optimized emission inventory uses East Asian anthropogenic emissions from *Streets et al.* [2003] and Eurasian anthropogenic emissions decreased by 50% from the *Wang et al.* [2003] inventory.
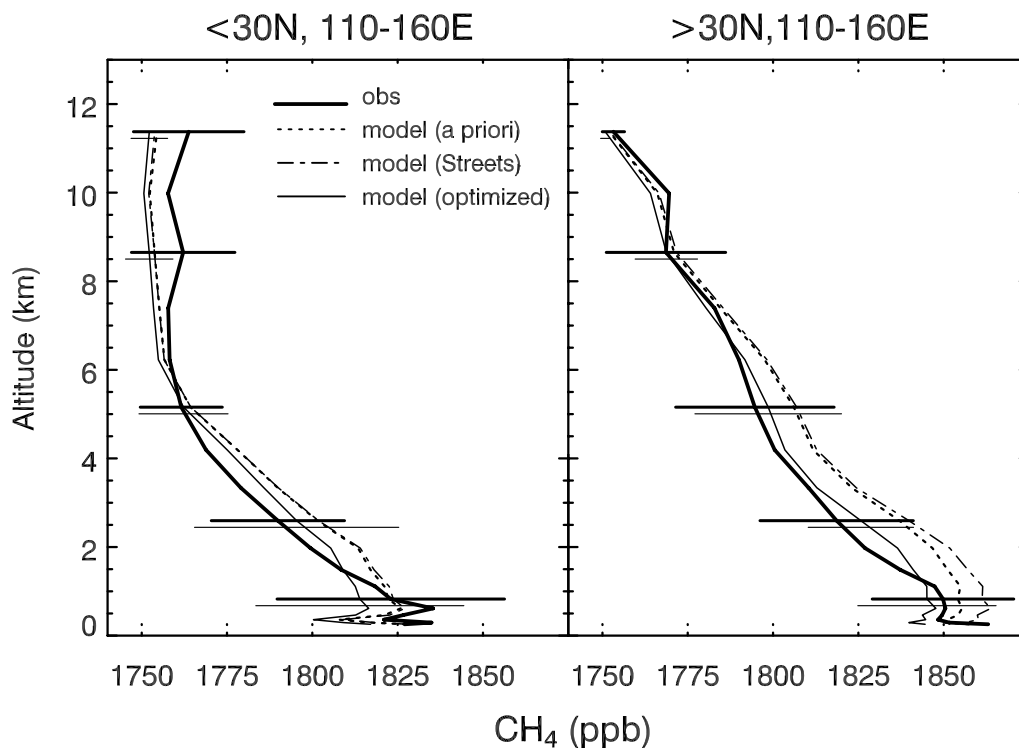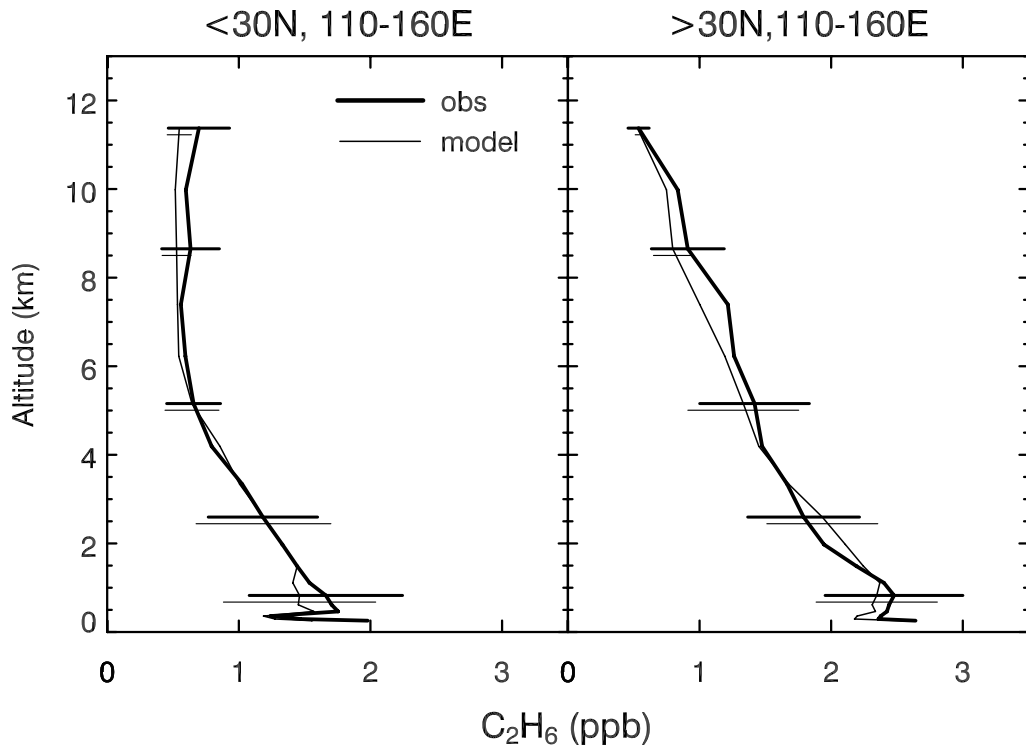
Figure 4b. Mean vertical profiles of CH$_4$ concentrations along the TRACE-P flight tracks, north of 30°N and south of 30°N at 110°E-160°E (NW Pacific, Asian outflow). Observations (thick lines) are compared to model values using the a priori emission inventory (dotted lines), the a priori inventory with anthropogenic East Asian sources from *Streets et al.* [2003] superimposed (dash-dotted lines), and the optimized emission inventory (solid lines). The a priori emission inventory is from *Wang et al.* [2003]. The optimized emission inventory uses East Asian anthropogenic emissions from *Streets et al.* [2003] and Eurasian anthropogenic emissions decreased by 50% from the *Wang et al.* [2003] inventory. The error bars show standard deviations (1σ) for the observations and the optimized model at selected levels.
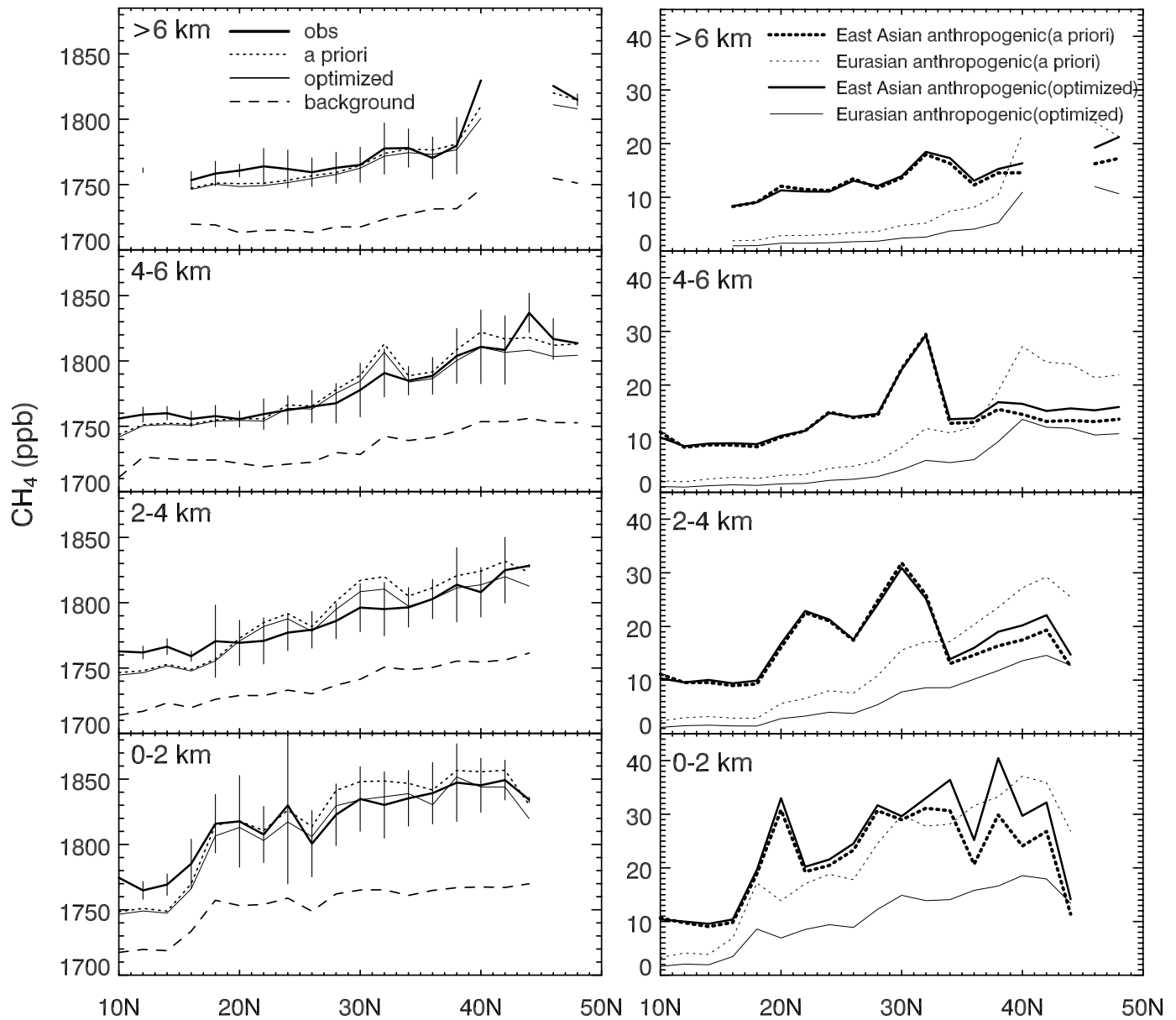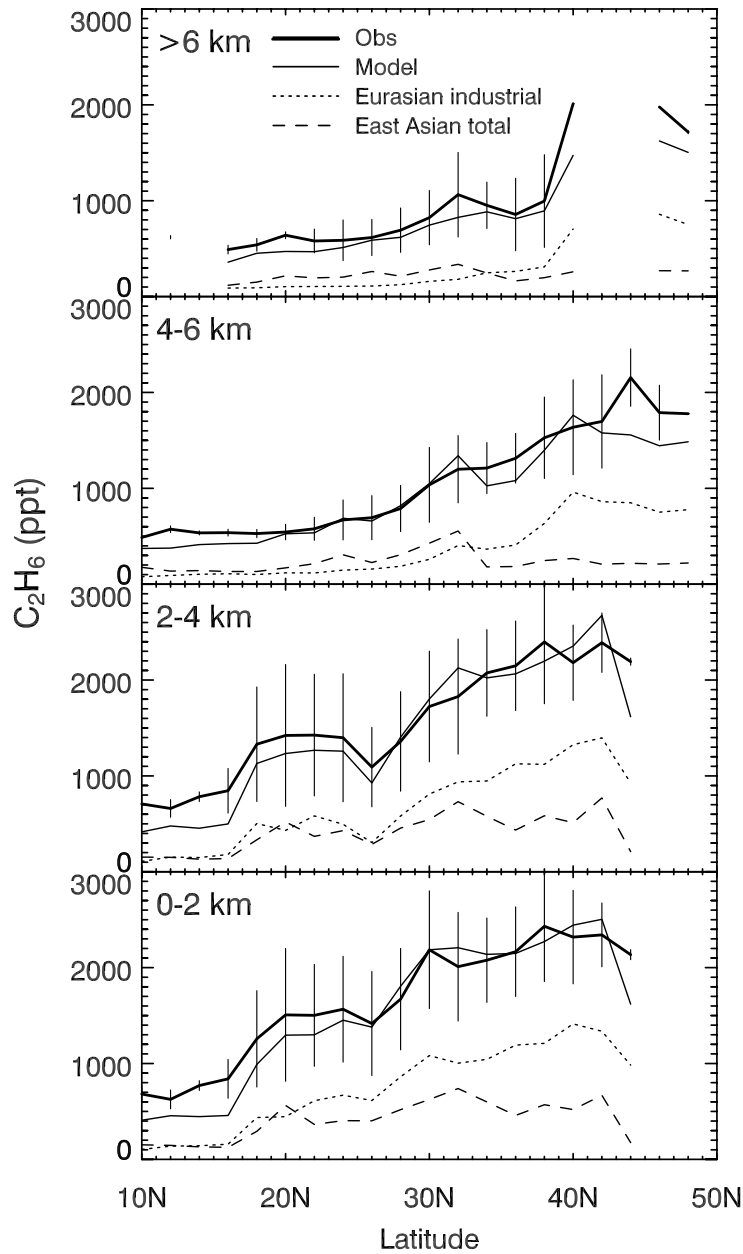
Figure 4c. Left panels: Latitudinal dependence of CH$_4$ concentrations along the TRACE-P flight tracks west of 160˚E and at different altitudes. Observations (thick lines) are compared to model results using a priori sources (dotted) and optimized sources (solid). Dashed lines indicate background CH$_4$ in the model (see text). The error bars represent standard deviations for the observations. Right panels: contributions from the anthropogenic East Asian and Eurasian tagged tracers to the CH$_4$ model fields using the a priori (dotted), and the optimized (solid) emission inventories. The a priori emission inventory is from *Wang et al.* [2003]. The optimized emission inventory uses East Asian anthropogenic emissions from *Streets et al.* [2003] and Eurasian anthropogenic emissions decreased by 50% from the *Wang et al.* [2003] inventory.
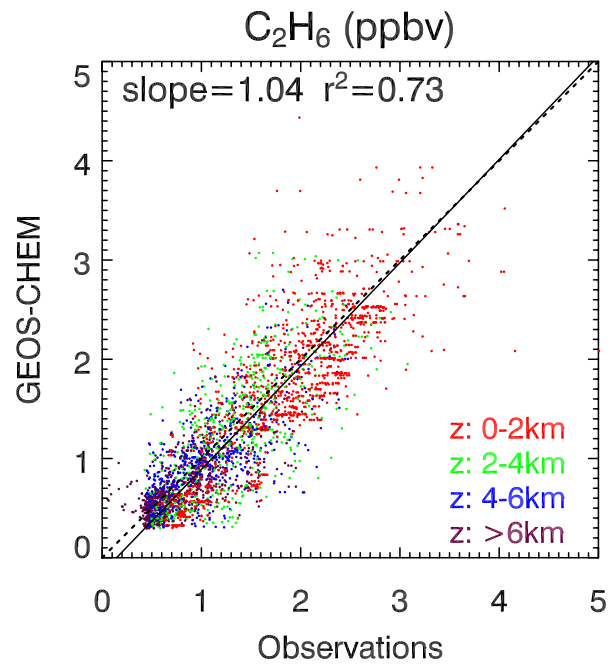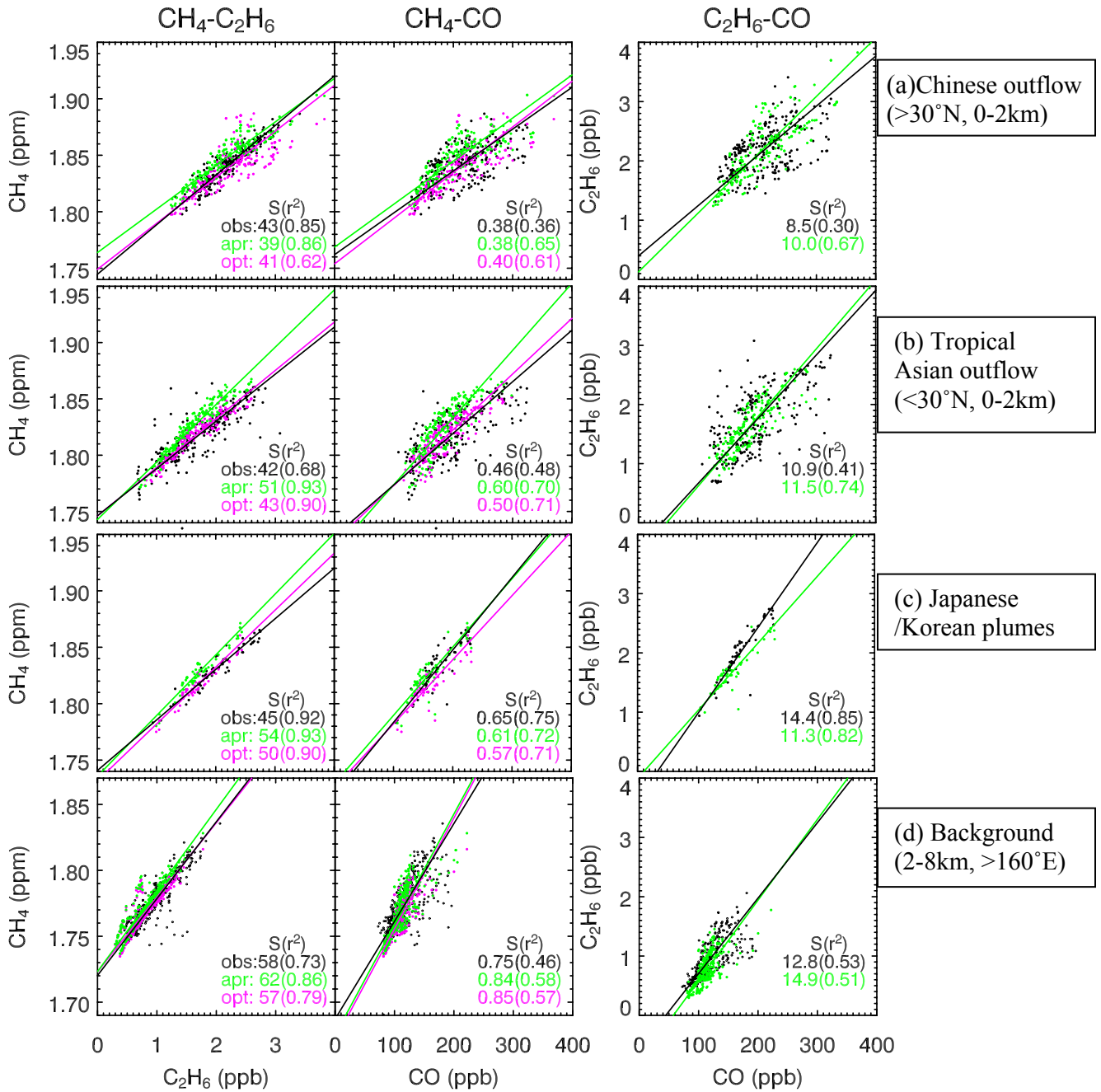
Figure 5a. Simulated vs. observed concentrations of C_2H_6 along the TRACE-P flight tracks over the northwest Pacific (west of 160˚E). The observations are averaged over the model grid boxes. The 1:1 line is shown as dotted. The solid line is the RMA regression line.

Figure 5b. Mean vertical profiles of C_2H_6 concentrations along the TRACE-P flight tracks, north of 30°N and south of 30°N at 110°E-160°E (NW Pacific, Asian outflow). Observations (thick lines) are compared to model values (solid lines). The error bars show the standard deviations for the observations and the model at selected levels.

Figure 5c. Latitudinal dependence of C_2H_6 concentrations along the TRACE-P flight tracks west of 160˚E during TRACE-P at different altitudes. Observations (thick lines) are compared to model results (solid lines). The error bars represent standard deviations for the observations. Contributions of C_2H_6 from East Asian (dashed) and Eurasian (dotted) tagged tracers in the model are also shown.

Figure 6. Simulated vs. observed CH_4-C_2H_6-CO correlations along the TRACE-P flight tracks in different regions. (a) Chinese outflow (>30˚N and <2km, west of 160˚E); (b) tropical Asian outflow (<30˚N and <2km, west of 160˚E); (c) Japanese/Korean plumes; (d) background (2-8km, east of 160˚E). TRACE-P observations ("obs", black) are compared to a priori model results ("apr", green) and optimized model results ("opt", red). The slopes (S) and r^2 of the RMA regression lines are shown (also in Table 3).
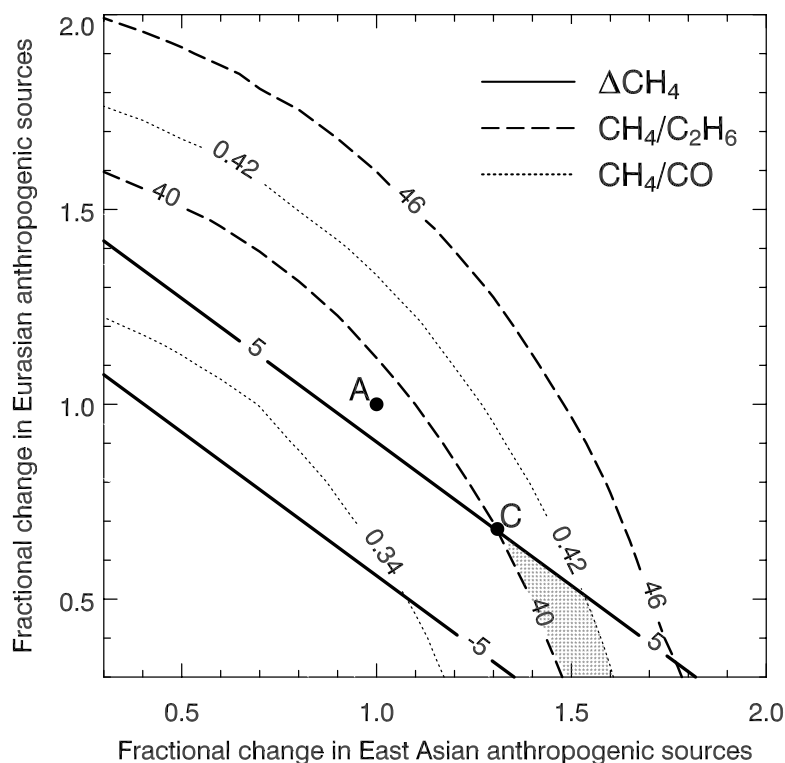
Figure 7. Constraints on East Asian and Eurasian CH_4 sources from the CH_4-C_2H_6-CO correlations observed in Asian outflow during the TRACE-P aircraft mission. The figure shows GEOS-CHEM model results for the slopes (mol mol^{-1}) of CH_4/C_2H_6 (dashed lines) and CH_4/CO (dotted lines), and the difference in ppb between simulated and observed CH_4 concentrations (solid lines), as a function of fractional changes of the East Asian and Eurasian anthropogenic sources of CH_4 relative to the a priori. Values are shown for the Chinese boundary layer outflow (north of 30°N and below 2 km altitude). The shaded region defines the range of emissions compatible with the TRACE-P observations; we require the model to match the observed CH_4 enhancement to within 5 ppb, and the observed CH_4/C_2H_6 and CH_4/CO slopes (43±3 mol mol^{-1} and 0.38±0.04 mol mol^{-1}, respectively) to within 95% confidence intervals (± 1.96σ). Point A (1, 1) represents the a priori emissions. Point C (1.3, 0.7) represents the minimum perturbation to the a priori emissions needed to fit the constraints from the TRACE-P observations: 30% increase and decrease of East Asian and Eurasian anthropogenic emissions respectively.